Journal Name

ARTICLE

Mesoporous Silica Nanoparticles Engineered for Ultrasound-Induced Uptake by Cancer Cells

Received 00th January 20xx,
Accepted 00th January 20xx

DOI: 10.1039/x0xx00000x

www.rsc.org/

Juan L. Paris[a,b], Miguel Manzano[a,b], M. Victoria Cabañas[a] and María Vallet-Regí[a,b,*]

A novel smart hierarchical ultrasound-responsive mesoporous silica nanocarrier for cancer therapy is here presented. This dynamic nanosystem has been designed to display different surface characteristics during its journey towards tumor cells. Initially, the anticancer-loaded nanocarriers are shielded with a polyethylene glycol layer. Upon exposure to high frequency ultrasound, the polymer shell detaches from the nanoparticles, exposing a positively-charged surface. That favors the internalization in human osteosarcoma cells, where release of topotecan takes place, drastically enhancing the cytotoxic effect.

Introduction

The use of nanoparticles in medicine, in the so-called nanomedicine, has the potential of drastically improving cancer diagnostics and therapy.[1] In this sense, the selective accumulation of nanoparticles in tumor tissues due to the Enhanced Permeation and Retention (EPR) effect has been used as the main rationale to develop nanoparticle-based drug delivery devices as therapeutic agents for cancer treatment,[2,3] some of which have already reached the market.[4] Grafting polyethylene glycol (PEG) chains on the surface of nanoparticles, a process known as PEGylation, has been proven as an effective way of increasing the circulation time of nanoparticles in the bloodstream, thereby allowing a higher dose of the nanocarrier to reach the tumor.[5] However, nanoparticle uptake by cells is hindered due to PEGylation.[5] Besides the passive accumulation of nanoparticles in tumor tissues due to the EPR effect, active targeting strategies have been extensively explored to improve the efficacy of nanomedicines.[2] However, active targeting is often accompanied by a series of disadvantages of its own. For example, PEGylated nanoparticles exposing targeting agents are withdrawn faster from systemic circulation than PEGylated nanoparticles without further modification.[6] This decrease in nanoparticle circulation time can indeed diminish the therapeutic efficacy of these nanocarriers. Additionally, the presence of targeting agents with a very high affinity for the target cells can also induce a paradoxical effect: cancer cells in the first line of the tumor tissue will interact with the nanoparticles in a very strong manner, retaining those particles in the periphery of the tumor and effectively preventing their distribution to deeper areas.[7] This effect has been called the "binding site barrier".

Hierarchical targeting strategies have been developed to overcome the above limitations of targeted nanomedicines.[6] In these hierarchical approaches, a targeting moiety is included in the formulation in a way that it remains hidden during nanoparticles transport along the bloodstream and it is later exposed once they reach the target tissue by passive accumulation. Cellular uptake of these materials can be triggered by a stimulus, either internal (such as pH or redox conditions)[8] or external (such as light).[9] In this context, pathological changes in internal conditions, like pH, are not very exacerbated.[10] Additionally, clinicians do not hold any control over the behavior of nanoparticles sensitive to internal stimuli. Nanoparticles sensitive to external stimuli can be more selective in their response, since they will only be activated by the voluntary application of the stimulus. However, the level of penetration in the tissue and potential damage to surrounding healthy tissues could be limitations for external stimuli. For example, light is known to penetrate poorly in solid tissues, even though Near Infrared light can be employed to improve this parameter.[10]

High frequency ultrasound can non-invasively penetrate very deep into tissues and is well tolerated by the body.[10] When an ultrasound (US) wave propagates through living tissues in the body, several thermal and mechanical effects occur, including pressure variation, acoustic fluid streaming, cavitation and local hyperthermia, and these effects can be used for different medical applications.[11] In these sense, we recently employed US to successfully trigger doxorubicin release from Mesoporous Silica Nanoparticles (MSNs) in cancer cells.[12] However, the use of ultrasound to trigger hierarchical targeting materials remains largely unexplored. The objective of the present work is to develop a nanoparticle

[a]Dpto. Química en Ciencias Farmacéuticas, Facultad de Farmacia, Universidad Complutense de Madrid, Instituto de Investigación Sanitaria Hospital 12 de Octubre i+12, 28040-Madrid, Spain.
[b]Centro de Investigación Biomédica en Red de Bioingeniería, Biomateriales y Nanomedicina (CIBER-BBN), Spain
*Corresponding author: vallet@ucm.es

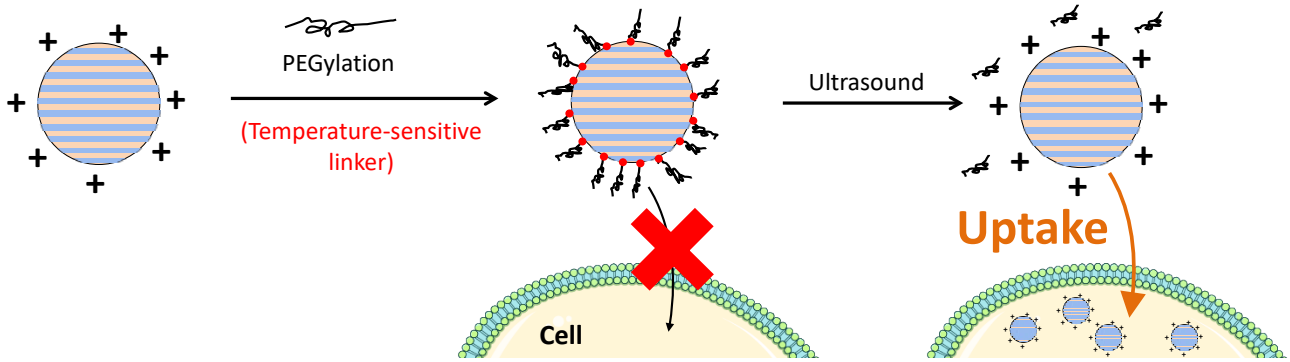

Scheme 1. Schematic representation of nanoparticle uptake by cells promoted by ultrasound-induced detachment of PEG shell from positively-charged MSNs.

that can undergo ultrasound-promoted uptake by cancer cells, by means of an ultrasound-induced temperature increase.

As a model nanoparticle we have selected MSNs due to their facile synthesis and functionalization and their high physicochemical stability.[13–15] Additionally, the textural properties of MSNs, such as their high surface area and pore volume, will provide high loading capacity of different drugs. Nanoparticle uptake by cells is generally enhanced by employing internalization ligands (targeting agents) or positively charged moieties on the surface of the nanoparticles.[6] We chose the exposure of a positively charged surface as the mechanism to induce cell internalization by using amine functionalized MSNs, due to the simplicity and broad applicability of this charge-dependent approach.[16] The positive charge on the nanoparticle surface will be hidden by grafting PEG chains on the nanoparticle surface through a thermosensitive linker. These PEG chains will be disengaged from the nanoparticles by subjecting the material to an ultrasound-induced temperature increase, exposing the positive charges of the particles. The concept of the material designed in this work is shown in **Scheme 1**.

Results and Discussion

It is well known that nanoparticle surface characteristics have a great importance in their interactions with biological environments. For example, PEGylation is known to increase the circulation time of nanoparticles.[5] However, cellular uptake in PEGylated nanoparticles is hindered.[5] On the other hand, nanoparticles with positively charged surfaces are generally internalized efficiently by cells (due to an electrostatic interaction with negatively-charged phospholipids in the cell membrane),[6,16] but their circulation time is much shorter. Therefore, the design of a nanosystem with different surface characteristics in the different delivery stages is here approached.

Mesoporous silica nanoparticles decorated with amino groups, MSN-NH_2, were used in our experiments. These positive nanoparticles were shielded, by decorating them with PEG, using 4,4'-azobis(4-cyanovaleric acid) (ABCVA) as linker (MSN-NH_2-T-PEG nanoparticles). ABCVA acts here as a thermosensitive linker, although it is commonly used as a radical initiator in polymer synthesis because it is cleaved when heated,[17] forming radical species that can start the polymerization.[12] In our case, the temperature increase by using US would induce the cleavage of the ABCVA linker,[18,19] separating PEG chains from the nanoparticle surface. PEGylated nanoparticles that are not thermosensitive (MSN-NH_2-PEG) were used as control and prepared by using succinic anhydride as a linker **(Scheme 2)**.

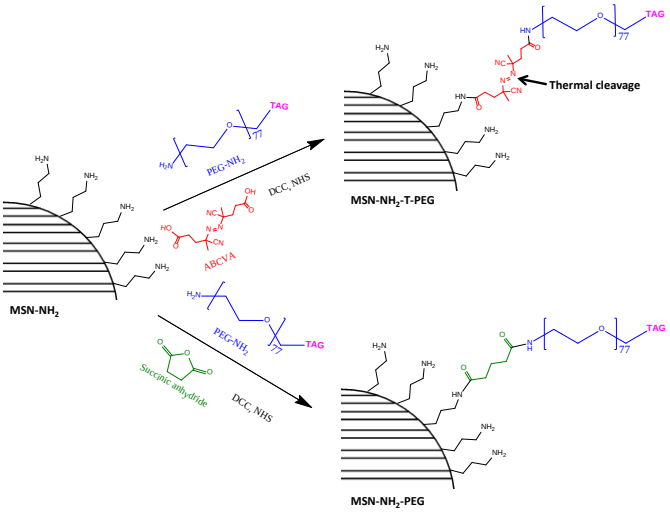

Scheme 2. Schematic representation of the preparation of MSN-NH2-T-PEG and MSN-NH2-PEG.

Samples were characterized before and after PEGylation. The Scanning Electron Microscopy (SEM) micrographs show that particle morphology (round-shaped) is maintained after PEG grafting (**Figure 1**). Small angle X-Ray Diffraction (XRD) patterns show that the ordered porous structure is maintained, although the intensity of the diffraction maxima decreases after PEG grafting, which is in agreement with previous results (Figure S1).[12] The Fourier-Transformed Infrared (FTIR) spectra of MSN-NH_2-PEG and MSN-NH_2-T-PEG show the presence of amide bonds in the material (*ca.* 1650 cm^{-1}), confirming the successful PEG grafting through amide bond formation to the nanoparticles (Figure S1). Thermogravimetric analysis (TGA) data indicate a percentage of organic matter due to PEG chains in the material of around 5.6 % and 5.2 % for MSN-NH_2-T-PEG

and MSN-NH_2-PEG, respectively (after subtracting the residual organic matter percentage present in MSN-NH_2 before PEG grafting). The amount of amino groups in MSN-NH_2 was $8.35x10^{-5}$ moles g^{-1} (as quantified by Fmoc UV assay). From the TGA data and knowing the molecular weight of the grafted PEG, the percentage of those amino groups occupied by PEG was estimated to be 18.2 % and 19.2 % for MSN-NH_2-PEG and MSN-NH_2-T-PEG, respectively. Z potential is modified from positive to negative values after PEGylation: +33.8 mV (MSN-NH_2), -32.1 mV (MSN-NH_2-PEG) and -30.2 mV (MSN-NH_2-T-PEG), indicating that the positive charge of the surface is hidden after the PEGylation process. Since most of the amino groups on the nanoparticle are not involved in the linkage to PEG, the drastic changes in the Z potential values must be attributed to a physical masking of the nanoparticle surface by the PEG chains.

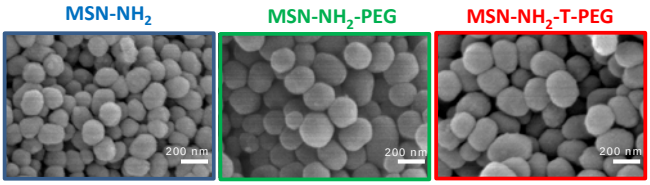

Figure 1. SEM micrographs of MSN-NH_2, MSN-NH_2-PEG and MSN-NH_2-T-PEG.

All of the above results confirm the successful masking of the nanoparticle surface by the PEGylation process. The system capacity to change its surface characteristics in response to stimuli was then evaluated step by step. First, we studied the PEG detachment after thermal and US treatments, then, the US-induced cellular uptake and finally, the cytotoxicity when the system was loaded with the anticancer drug topotecan.

The temperature responsiveness of the linker in our nanoparticles was evaluated through PEG chain detachment after thermal treatment. The PEG here employed (F-PEG-NH_2) was labeled with fluorescein to evaluate the fluorescence of the supernatant after treatment, which allowed the quantification of the PEG detached from our nanoparticles. Suspensions of MSN-NH_2-T-PEG and MSN-NH_2-PEG particles in phosphate-buffered saline (PBS, 1 mg mL^{-1}) were treated 70 ºC overnight to ensure complete cleavage of the ABCVA linker, and the supernatants obtained after centrifugation were analyzed by fluorimetry. A control experiment at physiological temperature (37 ºC) was performed simultaneously as a control. Figure 2 shows that fluorescence intensity was only detectable in the aqueous medium after MSN-NH_2-T-PEG suspension treatment at 70 ºC while no significant fluorescence was found in the supernatant of sample at 37 ºC. As expected, no fluorescence was observed in the samples with no thermosensitive linker (MSN-NH_2-PEG) independently of the temperature. These results show the thermoresponsive capacity of MSN-NH_2-T-PEG particles thanks to the presence of the selected linker which promotes the PEG detachment. After PEG detachment had been observed, the exposure of the positively-charged nanoparticle surface was evaluated. Z potential measurements after thermal treatment are in consonance with the fluorescence experiments, since only thermally-treated MSN-NH_2-T-PEG particles presented positive Z potential values (**Figure 2**).

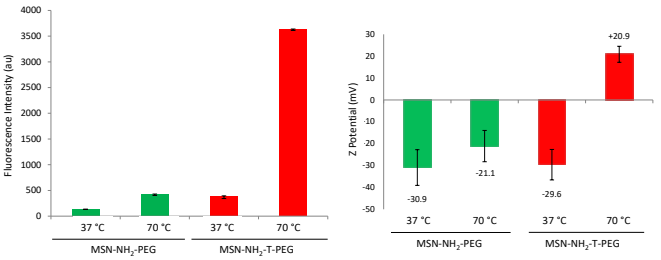

Figure 2. Fluorescence intensity of the supernatant of suspensions of MSN-NH2-PEG and MSN-NH2-T-PEG (obtained with FITC-labeled PEG) after thermal treatment at 70 ºC or control experiments at 37 ºC (left); Z potential measurements in water of the materials exposed to those same conditions (right).

Once the ability of this system to dissociate the PEG chains from its surface in response to temperature was confirmed, these materials were subjected to US as an external stimulus, to evaluate if a US-induced temperature increase could trigger that same behavior. **Figure 3** shows the fluorescence of the supernatant of MSN-NH_2-T-PEG and MSN-NH_2-PEG suspensions after US exposure for 20 min. Again, PEG fluorescence is only observed in the nanoparticles containing the thermosensitive linker, which means that the azo moiety in the ABCVA linker between PEG and MSN-NH_2 (Scheme 2) was cleaved in response to the temperature increase induced by US. It is worth mentioning that under the US conditions used, the macroscopic temperature of the solution was determined to be 48 ± 1 ºC (by a thermocouple placed in the setup during the experiments). Even though this temperature was above the range of therapeutic hyperthermia (40 -45 ºC),[20] it was much lower than the bulk temperature needed to induce the cleavage (70 ºC). This difference could be ascribed to a more intense localized heating in the nanoscale related to the occurrence of acoustic cavitation.[21] These results show that we have successfully developed a proof-of-concept material that can detach its PEG coating when exposed to an external energy source, such as 1.3 MHz ultrasound.

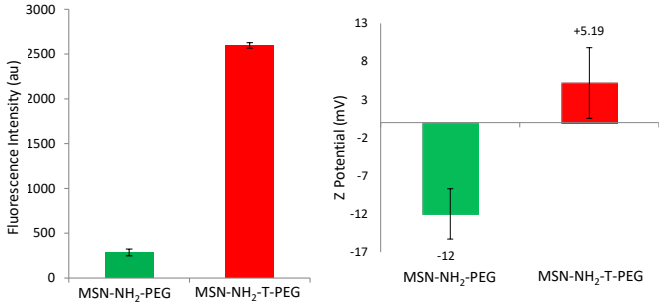

Figure 3. Fluorescence intensity of the supernatant of suspensions of MSN-NH2-PEG and MSN-NH2-T-PEG (obtained with FITC-labeled PEG) after US exposure (1.3 MHz, 100 W, 20 min) (left); Z potential measurements in water of the materials exposed to those same conditions (right).

The next step was to evaluate if this US treatment would be sufficient to provide a positively-charged surface. Thus, Z

potential measurements of the nanoparticles after US treatment were carried out (Figure 3). Positive values were only obtained after the US treatment of MSN-NH_2-T-PEG, while a negative charge was found in MSN-NH_2-PEG, in agreement with the absence of PEG detachment.

The results obtained by fluorimetry and Z potential measurements show that the application of an external stimulus as US provokes the detachment of the PEG chains from MSN-NH_2, inducing the exposure of protonated amino groups and, therefore, conferring a positively-charged surface to the nanoparticles.

The next step was to study if PEG detachment favors nanoparticle uptake. To evaluate that, MSN-NH_2-T-PEG and MSN-NH_2-PEG were exposed to US for 20 min prior to their incubation with HOS cells for 2 h. The cells were then washed with PBS to remove non-internalized nanoparticles and nanoparticle uptake was evaluated by fluorescence microscopy and flow cytometry (**Figure 4**).

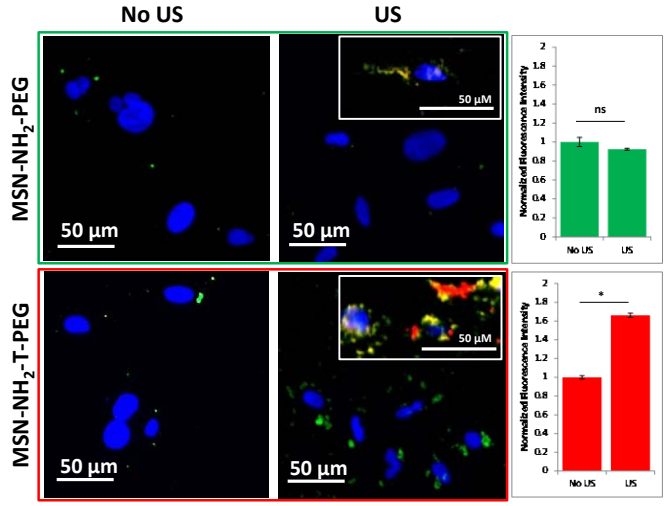

Figure 4. Fluorescence microscopy images (left) and flow cytometry data (right) of osteosarcoma cells (HOS) incubated with MSN-NH2-PEG and MSN-NH2-T-PEG exposed or not to ultrasound. Blue fluorescence shows stained nuclei with DAPI, green fluorescence shows MSN core and red fluorescence (inserts in right images) shows PEG chains. ns= no significant differences; *p<0.05.

In this experiment, we employed FITC labeled MSN-NH_2 and RBITC-labeled PEG chains. The results indicate a higher cellular uptake of MSN-NH_2-T-PEG nanoparticles that had been exposed to ultrasound than in any of the other experimental groups, in agreement with the surface charge reversion of the nanoparticles after the US-induced temperature increase. Moreover, a partial lack of co-localization between red and green fluorescence in the ultrasound-exposed MSN-NH_2-T-PEG sample indicates the detachment of PEG chains from the nanoparticles (Insert in Figure 4), in agreement with previous *in vial* experiments above shown. For ultrasound-exposed MSN-NH_2-PEG under the same conditions, red and green fluorescence overlap, indicating that PEG chains are still attached to the nanoparticles (Insert in Figure 4). To ensure that the nanoparticles are internalized by the cells, flow cytometry was performed in cells suspensions in trypan blue solution, to remove extracellular fluorescence. Normalized fluorescence intensity of the cells determined by flow cytometry (Figure 4) shows a significant increase in MSN-NH_2-T-PEG uptake after US exposure, while no significant differences were found by ultrasound application for MSN-NH_2-PEG.

Once the nanoparticles are internalized by the tumor cells after US stimulus, they should be able to induce their death. The therapeutic potential of our system was therefore evaluated with a cytotoxicity study, employing topotecan-loaded nanoparticles. Topotecan is a water-soluble cytotoxic drug (classified as a topoisomerase 1 inhibitor, an analog of camptothecin). The use of nanocarriers that can release the drug in the intracellular compartment leads to very high concentrations of the drug, increasing the efficacy of the platform. Therefore, relative levels of cell death obtained with different nanocarrier formulations in the same cell line could also be an indicator of the degree of internalization of the different materials studied. To carry out the cytotoxicity experiments, topotecan-loaded nanoparticles were incubated with HOS cells following the same protocol as the one employed for the uptake experiments (incubation for 2 h in complete culture medium after 20 min US pretreatment). Cell viability was evaluated at two different time points: 2 or 24 h since the removal of non-internalized nanoparticles. The results of this cell viability study **(Figure 5**) show that significant cell death is only observable with US-exposed TOP-MSN-NH_2-T-PEG, while under all of the other conditions, the cells remained viable. These data are in agreement with the nanoparticle uptake experiments, since the nanoparticle uptake was much less efficient in absence of thermolinker and/or US application.

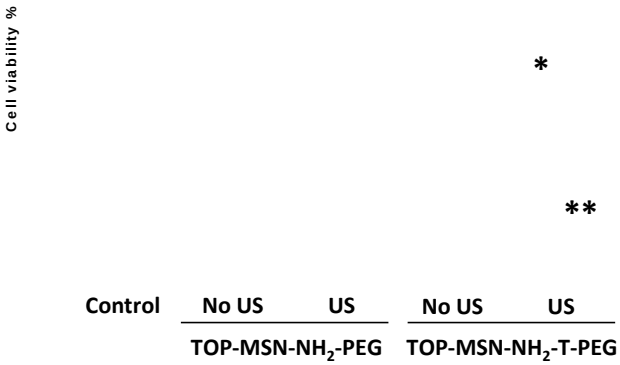

Figure 5. Cell viability of HOS cells (evaluated by Alamar Blue test) incubated with TOP-MSN-NH2-PEG and TOP-MSN-NH2-T-PEG with or without prior US application. *p<0.05; **p<0.001 (compared to control).

All of the results here presented confirm the fabrication of a smart hierarchical nanoparticle. Initially, the material presents a PEGylated surface, which allows it to circulate in the

bloodstream until it is accumulated in the tumor tissue by the EPR effect. Once the tumor is reached, the nanosystem would change its surface properties in response to the application of an external stimulus, enabling a more effective interaction with the cancer cells that would lead to nanoparticle uptake.

The results obtained in this work highlight a great potential for ultrasound-induced nanoparticle uptake. Shielding active targeting molecules on the nanoparticle surface and exposing them only after the application of external stimuli by analogous strategies could also improve the specificity of this kind of approaches.

Conclusions

We have successfully synthesized a smart hierarchical system by developing a PEGylated Mesoporous Silica Nanoparticle capable of undergoing detachment of the PEG chains under US treatment. The application of an external stimulus such as US is also capable of displaying positively-charged surface of the nanoparticle.

The exposure of the positively-charged surface induced by ultrasound treatment enhanced the cellular uptake of the nanoparticles, while the application of ultrasound in a control material did not induce any changes in its uptake. Finally, US-promoted nanoparticle uptake greatly increased the toxicity of topotecan-loaded nanoparticles in human osteosarcoma cells.

Experimental section

Materials

The following compounds were purchased from Sigma-Aldrich Inc. (Spain): Ammonium nitrate, cetyltrimethylammonium bromide (CTAB), tetraethyl orthosilicate (TEOS), (3-aminopropyl)triethoxysilane (APTES), 9-Fluorenylmethoxycarbonyl (Fmoc) chloride, piperidine, poly(ethylene glycol) bis(amine) average M_n 3400 Da (NH_2-PEG-NH_2), dimethylformamide (DMF), N-hydroxysuccinimide (NHS), succinic anhydride, 4,4'-azobis(4-cyanovaleric acid) (ABCVA), N,N'-dicyclohexylcarbodiimide (DCC), phosphate-buffered saline (PBS), rhodamine-B isothyocianate (RBITC), fluorescein isothyocianate (FITC) and topotecan hydrochloride hydrate (TOP). Dulbecco's Modified Eagle's Medium (DMEM), penicillin-streptomycin, non-essential aminoacids, trypsin-EDTA were purchased from Invitrogen (Fisher Scientific, Spain). Fetal bovine serum is from Biowest (Labclinics, Spain). These compounds were used without further purification.

Characterization Techniques

The materials were analyzed by small angle X-ray diffraction (XRD) in a Philips X'Pert Multipurpose Diffractometer (MPD) equipped with Cu Kα radiation. Fourier transformed infrared (FTIR) spectra were obtained in a Nicolet Nexus spectrometer (Thermo Fisher Scientific) equipped with a Smart Golden Gate attenuated total reflectance (ATR) accessory. Thermogravimetry and differential thermal analysis (TGA/DTA) were performed in a PerkinElmer Pyris Diamond TG/DTA analyzer, with 10 ºC/min heating ramps, from room temperature to 600 ºC. ^{1}H NMR experiments were carried out in a Bruker AV 250 MHz apparatus. Surface morphology was analyzed by scanning electron microscopy (SEM) in a JEOL 6400 electron microscope. Z potential was measured in deionized water by means of a Zetasizer Nano ZS (Malvern Instruments) equipped with a 633 nm "red" laser. Fluorescence spectrometry was used to determine PEG detachment by means of a Biotek Synergy 4 device. Fluorescence microscopy was performed with an Evos FL Cell Imaging System equipped with three Led Lights Cubes (λ_{EX} (nm); λ_{EM} (nm)): DAPI (357/44; 447/60), GFP (470/22; 525/50), RFP (531/40; 593/40) from AMG (Advance Microscopy Group). Quantitative analysis of cellular uptake was performed by flow cytometry (FACS) in a BD FACSCalibur™ cytometer, and results were processed using Flowing Software. Ultrasound experiments were performed in a commercial laboratory ultrasound apparatus (RBI, France), working at 1.3 MHz and 100 W for 20 min, following similar conditions as those described in our previous work.[12]

Synthesis of PEGylated Mesoporous Silica Nanoparticles

Amino-functionalized mesoporous silica nanoparticles (MSN-NH_2) were obtained by a modified Stöber method from a mixture of TEOS and APTES (90:10 molar ratio) in the presence of CTAB as structure-directing agent under basic and very dilute conditions, as described elsewhere.[16] MSN-NH_2 labeled with FITC were also obtained by reacting 1 mg of FITC with 2.2 µL APTES in 100 µL ethanol for 2 h. Then, the reaction mixture was added with the TEOS and APTES solution as already described.

The quantification of amino groups available on MSN-NH_2 was performed by a Fmoc UV assay,[22] based on the reaction of Fmoc chloride with the amino groups to be quantified. Briefly, 50 mg of MSN-NH_2 were mixed with 125 mg of Fmoc chloride (excess), purged with nitrogen and dissolved in 3 mL of dry DMF under inert atmosphere. That solution was magnetically stirred overnight at room temperature. Then, the material was collected by centrifugation and washed with DMF, water (3 times) and ethanol (twice) to get rid of unbounded Fmoc. That material was dried under vacuum. Different portions were weighted and dispersed in 1 mL of a solution of 20 % piperidine in DMF to deprotect the amino groups and release the Fmoc from the material. That reaction was performed under sonication for 20 min. After centrifugation, the absorbance of the supernatant at 301.5 nm was measured, and the amount of Fmoc released from the amines was measured. Once the amount of Fmoc released was known, the amount of amino groups per mg of material was extrapolated (molar ratio 1:1).

Before the PEGylation process, commercial NH_2-PEG-NH_2 was labeled with FITC (F-PEG-NH_2) or RBITC (R-PEG-NH_2) in order to be detected by green and red fluorescence, respectively. F-PEG-NH_2 was obtained by reacting 100 mg of NH_2-PEG-NH_2 with 11 mg of FITC (1:1 molar ratio) in 5 mL of dry DMF under

inert atmosphere (N_2). The reaction was carried out at room temperature under magnetic stirring overnight (under inert atmosphere). Then, the reaction products were precipitated in diethyl ether and dried at room temperature. The products were dissolved in water and F-PEG-NH_2 was purified by size exclusion chromatography (Sephadex® G-25). ^{1}H NMR spectra of different fractions after liophylization were performed to select the desired product. R-PEG-NH_2 was obtained in a similar way, but using 16 mg of RBITC instead of FITC (to maintain the 1:1 molar ratio).

MSN-NH_2 functionalization with PEG was carried out through DCC/NHS chemistry using a thermosensitive linker such as ABCVA to obtain thermosensitive PEGylated nanoparticles (MSN-NH_2-T-PEG). Similar protocol was followed with succinic anhydride as a linker to prepare non-thermosensitive PEGylated nanoparticles (MSN-NH_2-PEG) to be used as control.

To obtain MSN-NH_2-T-PEG, 1.6 mg of ABCVA were activated with 3.4 mg of DCC and 1.9 mg of NHS in 2 mL of dry DMF under inert atmosphere with magnetic stirring at room temperature for 30 min. Then, 20 mg of F-PEG-NH_2 (or R-PEG-NH_2) dissolved in 1 mL of dry DMF were added and stirred for 2 h at room temperature (molar ratio of 1:1 with ABCVA). Finally, 20 mg of MSN-NH_2 nanoparticles dispersed in 1 mL of dry DMF were added. The reaction medium was stirred overnight and the product was collected by centrifugation and washed with DMF twice and with water 3 times. The material was then dried under vacuum.

To obtain MSN-NH_2-PEG, 20 mg of F-PEG-NH_2 (or R-PEG-NH_2) and 0.6 mg of succinic anhydride were dissolved in 2 mL of dry DMF under inert atmosphere, and the mixture was magnetically stirred at room temperature for 1.5 h. Then, 1.8 mg DCC and 1 mg of NHS dissolved in 1 mL of dry DMF were added and stirred for other 2 h. Then, 20 mg of MSN-NH_2 nanoparticles dispersed in 1 mL of dry DMF were added and reacted overnight. The material was purified as described above for MSN-NH_2-T-PEG.

Evaluation of stimuli-responsive PEG detachment from the material

To evaluate the detachment of PEG chains from MSN-NH_2-PEG or MSN-NH_2-T-PEG, nanoparticles with FITC-labeled PEG chains were employed. Several 1 mL aliquots of suspensions of those materials in PBS (1 mg mL^{-1}) were placed in an oven and subjected to two different thermal treatments: 37 ºC or 70 ºC overnight (samples were sealed to prevent any solvent evaporation). Additionally, suspensions of both nanoparticle types were exposed to US by using a commercial laboratory ultrasound apparatus working at 1.3 MHz and 100 W for 20 min. A thermocouple was introduced in the experimental setup during the ultrasound application experiments to evaluate the temperature rise induced by the stimulus.

After the different treatments, the suspensions were centrifuged (10000 rpm, 10 min). The supernatants were analyzed by fluorimetry to determine the presence of F-PEG-NH_2 detached from the materials. The materials were washed 3 times with PBS, dried and stored until further analysis. Z potential from those materials was performed in aqueous suspension to evaluate any changes on the surface charge of the materials after the different treatments.

***In vitro* nanoparticle uptake and cancer cell killing**

Human Osteosarcoma (HOS) cells were seeded in 24 well plates at a density of around 20,000 cells cm^{-2} 24 h before the experiments were carried out. Cells were grown in DMEM supplemented with 2mM of glutamine, 1 % penicillin/streptomycin and 10 % fetal bovine serum, at 37 ºC, 5 % CO_2 and 95 % humidity.

Nanoparticle uptake by HOS cells was evaluated by fluorescence microscopy employing nanoparticles prepared with RBITC-labeled PEG and FITC-labeled MSN-NH_2. Thus, the location of both MSN-NH_2 and PEG could be traced with the microscope. HOS cells were exposed to a suspension of MSN-NH_2-T-PEG or MSN-NH_2-PEG (without or with 20 min US pretreatment in both cases) in DMEM culture medium (200 μg mL^{-1}) for 2 h. Then, the cells were washed with PBS twice and then fixed with a solution of DAPI in methanol. That medium was changed with PBS to perform fluorescence microscopy.

Quantitative analysis of cellular uptake was performed by flow cytometry. HOS cells were incubated with the nanoparticles in complete culture medium (200 μg mL^{-1}) for 2 h, and after washing out non-internalized nanoparticles with PBS, the cells were trypsinised, collected by centrifugation and redispersed in PBS solution with trypan blue (0.5 %) to remove extracellular fluorescence. The fluorescence intensity of 10,000 cells was quantified by flow cytometry. Statistical analysis for differences between groups was carried out by the Student's *t* test.

Nanoparticles were loaded with topotecan, an anticancer drug, to carry out cytotoxicity experiments. Drug loading was performed by dispersing MSN-NH_2-PEG, or MSN-NH_2-T-PEG, in a solution of topotecan (2 mg mL^{-1} in PBS), and magnetically stirring them overnight at room temperature. Those nanoparticles containing topotecan, TOP-MSN-NH_2-PEG and TOP-MSN-NH_2-T-PEG, were collected by centrifugation and washed with PBS 3 times. Incubation of HOS cells with these nanoparticles (without or with 20 min US pretreatment) was performed in complete culture media as described above for the internalization experiments (2 h of incubation time). After washing out non-internalized nanoparticles with PBS, cell viability was evaluated at different time points (2 and 24 h) by a commercial Alamar Blue test (Invitrogen, Spain), following the manufacturer's instructions. Statistical analysis was carried out using the Student´s *t* test.

Conflicts of interest

There are no conflicts to declare.

Acknowledgements

The authors thank the funding from the European Research Council through the Advanced Grant VERDI (ERC-2015 AdG

proposal no. 694160). Financial support from Ministerio de Economía y Competitividad, (MEC), Spain (Project MAT2015-64831-R) is gratefully acknowledged. JL Paris gratefully acknowledges MEC, Spain, for his PhD grant (BES-2013-064182).

References

1 G. Chen, I. Roy, C. Yang and P. N. Prasad, *Chem. Rev.*, 2016, **116**, 2826–2885.
2 H. Maeda, H. Nakamura and J. Fang, *Adv. Drug Deliv. Rev.*, 2013, **65**, 71–79.
3 N. Bertrand, J. Wu, X. Xu, N. Kamaly and O. C. Farokhzad, *Adv. Drug Deliv. Rev.*, 2014, **66**, 2–25.
4 C. M. Dawidczyk, C. Kim, J. H. Park, L. M. Russell, K. H. Lee, M. G. Pomper and P. C. Searson, *J. Control. Release*, 2014, **187**, 133–144.
5 H. Hatakeyama, H. Akita and H. Harashima, *Biol. Pharm. Bull.*, 2013, **36**, 892–899.
6 S. Wang, P. Huang and X. Chen, *Adv. Mater.*, 2016, **28**, 7340–7364.
7 V. P. Chauhan and R. K. Jain, *Nat. Mater.*, 2013, **12**, 958–962.
8 A. Bandekar, C. Zhu, A. Gomez, M. Z. Menzenski, M. Sempkowski and S. Sofou, *Mol. Pharm.*, 2013, **10**, 152–160.
9 A. Barhoumi, W. Wang, D. Zurakowski, R. S. Langer and D. S. Kohane, *Nano Lett.*, 2014, **14**, 3697–3701.
10 S. Mura, J. Nicolas and P. Couvreur, *Nat. Mater.*, 2013, **12**, 991–1003.
11 A. K. W. Wood and C. M. Sehgal, *Ultrasound Med. Biol.*, 2015, **41**, 905–928.
12 J. L. Paris, M. V. Cabañas, M. Manzano and M. Vallet-Regí, *ACS Nano*, 2015, **9**, 11023–11033.
13 A. Baeza, M. Manzano, M. Colilla and M. Vallet-Regí, *Biomater. Sci.*, 2016, **4**, 803–813.
14 M. Manzano, M. Colilla and M. Vallet-Regí, *Expert Opin. Drug Deliv.*, 2009, **6**, 1383–1400.
15 M. Vallet-Regí, A. Rámila, R. P. del Real and J. Pérez-Pariente, *Chem. Mater.*, 2001, **13**, 308–311.
16 J. L. Paris, P. de la Torre, M. Manzano, M. V. Cabañas, A. I. Flores and M. Vallet-Regí, *Acta Biomater.*, 2016, **33**, 275–82.
17 H. Yorimitsu, K. Wakabayashi, H. Shinokubo and K. Oshima, *Bull. Chem. Soc. Jpn.*, 2001, **74**, 1963–1970.
18 P. Saint-Cricq, S. Deshayes, J. I. Zink and A. M. Kasko, *Nanoscale*, 2015, **7**, 13168–13172.
19 K. L. Berkowski, S. L. Potisek, C. R. Hickenboth and J. S. Moore, *Macromolecules*, 2005, **38**, 8975–8978.
20 P. Wust, B. Hildebrandt, G. Sreenivasa, B. Rau, J. Gellermann, H. Riess, R. Felix and P. Schlag, *Lancet Oncol.*, 2002, **3**, 487–497.
21 I. Rosenthal, J. Z. Sostaric and P. Riesz, *Ultrason. Sonochem.*, 2004, **11**, 349–363.
22 C. Kay, O. E. Lorthioir, N. J. Parr, M. Congreve, S. C. McKeown, J. J. Scicinski and S. V. Ley, *Biotechnol. Bioeng.*, 2000, **71**, 110–118.